

# Thermal Anisotropy Enhanced by Phonon Size Effects in Nanoporous Materials

Giuseppe Romano and Alexie M. Kolpak

*Department of Mechanical Engineering, Massachusetts Institute of Technology,  
77 Massachusetts Avenue, Cambridge, MA 02139\**

While thermal anisotropy is a desirable materials property for many applications, including transverse thermoelectrics and thermal management in electronic devices, it remains elusive in practical natural compounds. In this work, we show how nanoporous materials with anisotropic pore lattices can be used as a platform for inducing strong heat transport directionality in isotropic materials. Using density functional theory and the phonon Boltzmann transport equation, we calculate the phonon-size effects and thermal conductivity of nanoporous silicon with different anisotropic pore lattices. Our calculations predict a strong directionality in the thermal conductivity, dictated by the difference in the pore-pore distances along the two Cartesian axes. As the space between pores along the direction of the applied temperature gradient represents the phonon bottleneck, an anisotropic pores lattice distortion induces directionality in heat transport. Using Fourier's law, we also compute diffusive heat transport for the same geometries obtaining significantly smaller anisotropy, revealing the crucial role of phonon-size effects in tuning thermal transport directionality. Besides enhancing our understanding of nanoscale heat transport, our results demonstrate the promise of nanoporous materials for modulating anisotropy in thermal conductivity.

October 13, 2016

## INTRODUCTION

Designing materials to achieve desired thermal properties is pivotal for many modern applications, including thermoelectrics [1] and heat management in electronic devices [2]. Use of nanostructures has led to the achievement of new extremes in both high and low thermal conductivities relative to natural materials [3]. The degree of transport suppression is dictated by the relationship between the characteristic length of the material and the dominant phonon mean free path (MFP) [4]. For example, recent experiments have demonstrated very low thermal conductivities in thin films [5], nanowires [6, 7], and porous materials [8–11], illustrating the effectiveness of boundary engineering in tuning thermal transport [12].

While suppression of phonon transport in nanostructured materials has recently attracted a great deal of attention, little is known about the directionality of thermal conductivity in such materials. Thermal anisotropy, i.e., directional-dependent heat transport, is a desirable property for transverse thermoelectrics, in which electron and phonon flows are orthogonal to each other [13]. In-plane anisotropic thermal conductivities have been demonstrated in layered two-dimensional (2D) materials such as arsenene [14] and phosphorene [15], which also exhibit promising thermoelectric properties. In these systems, the in-plane directionality of heat transport arises from the puckered nature of the structures. In general, however, materials with both native anisotropic thermal transport and practical thermoelectric efficiencies remain elusive. The wide range of pore sizes and configurations that have been demonstrated [12, 16–18] suggest that nanoporous materials are a good platform for artificially

inducing and tuning thermal anisotropy in isotropic materials. In this work, we investigate this possibility using nanoporous silicon as a text case. Using our recently developed approach based on the Boltzmann Transport Equation (BTE) [16], we calculate the phonon-size effects and the thermal conductivity tensor in nanoporous silicon with anisotropic pore lattices. We consider two different pore arrangements: the configuration with fixed pore size and the case where the pore size is adjusted to keep the porosity fixed. For all the configurations, we observe a significant thermal conductivity anisotropy. These findings can be explained in terms of the directionality of the phonon bottleneck, represented by the pore-pore distance along the applied temperature gradient. On the other side, simple Fourier's law simulations for the same geometries predict weak anisotropy, revealing the importance of phonon-size effects in enhancing thermal transport directionality.

Thermal transport simulations are performed over a unit-cell with size  $L_x \times L_y$  comprising a single square pore of size  $L_p$ , as shown in Fig. 1(a). The pore lattice is identified by the orthogonal lattice vectors  $\mathbf{a}_1 = L_y r \hat{\mathbf{x}}$  and  $\mathbf{a}_2 = L_y \hat{\mathbf{y}}$ , where  $r$  is the shape factor, simply defined as  $r = L_x / L_y$ . The size of the unit-cell along  $y$  is  $L_y = 10$  nm. For an arbitrary  $r$ , the porosity, i.e. the ratio between the area of the pore and the area of the unit-cell, is simply  $\phi(r) = L_p^2 / (r L_y^2)$ . The chosen porosity for the square lattice, i.e.  $r = 1$  is  $\phi(1) = 0.25$ , which leads to the pore side  $L_p = 5$  nm. The thermal conductivity tensor is reconstructed by applying a difference of temperature  $\Delta T = 1$  K along the Cartesian axis  $\alpha$  and collecting heat flux along the same direction. Then, the application of Fourier's law gives  $\kappa_{\alpha\alpha} = \frac{L_\alpha}{\Delta T} \int_{C_\alpha} \mathbf{J}(\mathbf{r}, \Lambda, \Omega) \cdot \mathbf{n} dS$ , where  $C_\alpha$  is the boundary of the unit-cell with normal aligned with  $\alpha$ . The off-diagonal terms of thermal conductivity tensor are zero because of the symmetry of the system.

In absence of phonon size effects, heat transport is governed by the diffusive heat conduction equation, i.e.  $\kappa_{bulk} \nabla^2 T(\mathbf{r}) = 0$ , where  $\kappa_{bulk}$  is the bulk thermal conductivity. Within Fourier's law, thermal flux is simply  $\mathbf{J}(\mathbf{r}) = -\kappa_{bulk} \nabla T(\mathbf{r})$ . For a square pore lattice, which we will refer to as the "isotropic case", the Maxwell-Garnett theory predicts the reduction in the diffusive heat transport  $\kappa/\kappa_{bulk} \approx f(\phi) = (1-\phi)/(1+\phi)$  [19]. This configuration corresponds to the case with  $r = 1$ , which leads to  $\kappa_{xx} = \kappa_{yy} \approx 90 \text{ Wm}^{-1}\text{K}^{-1}$ . In order to investigate thermal transport in anisotropic pore lattices, we first perform simulations with fixed pores size and with shape factors  $r = 1, 2, 3$ . For larger  $r$ , the four-fold symmetry is broken and  $\kappa_{xx} \neq \kappa_{yy}$ , as shown in Fig. 2(a). As larger  $r$  results in smaller porosities, both  $\kappa_{xx}$  and  $\kappa_{yy}$  increase with the the shape ratio, with  $\kappa_{yy}$  being higher than  $\kappa_{xx}$  because of the higher material removal *seen* along  $\hat{\mathbf{y}}$ . We also plot the equivalent isotropic thermal conductivity as a function of  $r$ , i.e.  $\kappa = \kappa_{bulk} f(\phi(r))$ , which results in a curve living between  $\kappa_{xx}$  and  $\kappa_{yy}$ . In the next section, we will analyze the influence of phonon-boundary scattering on the thermal conductivity tensor.

Phonon-size effects are computed by solving the BTE which, under the relaxation time approximation, reads as

$$\Lambda \mathbf{s}(\Omega) \cdot \nabla T(\mathbf{r}, \Lambda, \Omega) + T(\mathbf{r}, \Lambda, \Omega) = \gamma \int_0^\infty \frac{K(\Lambda)}{\Lambda^2} \langle T(\mathbf{r}, \Lambda, \Omega) \rangle d\Lambda, \quad (1)$$

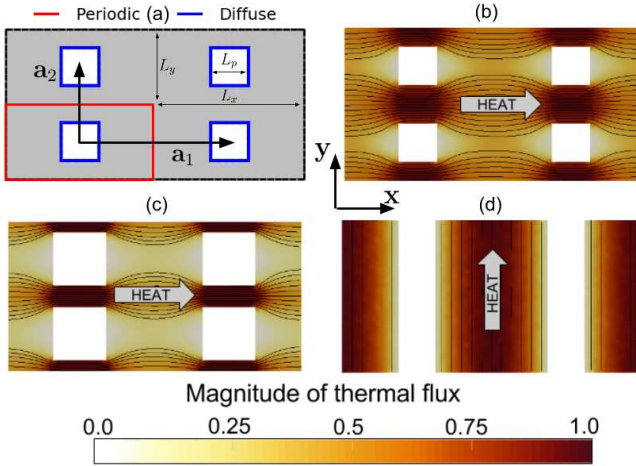


FIG. 1. a) The simulation domain comprises one single square pore. Periodic boundary conditions are applied both along  $x$ - and  $y$ -directions. The walls of the pores are assumed to be diffusive. Magnitude of thermal flux when a temperature gradient is applied along the  $x$ -direction for a shape ratio  $r = 2$  and porosity b)  $\phi = 0.125$  (fixed-pore case) and c)  $\phi = 0.25$  (fixed-porosity case). d) The thermal flux map for the thin-film limit case, where the applied temperature gradient is along  $y$ .

where  $T(\mathbf{r}, \Lambda, \Omega)$  is the effective temperature associated with phonons with MFP  $\Lambda$  and direction  $\mathbf{s}(\Omega)$ ,  $\langle \cdot \rangle$  is an angular average and  $\gamma$  is a material property, defined as  $\gamma = \int_0^\infty K(\Lambda)/\Lambda d\Lambda$ . The term  $K(\Lambda)$  is the bulk MFP distribution, computed by the density functional theory. [20, 21]. Eq. 1 is discretized in space by means of the finite-volume method [22] and in angular domain by the discrete ordinate method [23]. Periodic boundary conditions are applied along both  $\hat{\mathbf{x}}$  and  $\hat{\mathbf{y}}$ , while the walls of the pores are assumed to scatter phonon diffusively. This condition is achieved by enforcing zero normal flux along the pore's wall, which leads to the following condition on the boundary temperature [24]

$$T_b = - \frac{\int_0^\infty \int_{\mathbf{s}(\Omega) \cdot \mathbf{n} \geq 0} \mathbf{J}(\mathbf{r}, \Lambda, \Omega) \cdot \mathbf{n} d\Omega d\Lambda}{\int_{\mathbf{s}(\Omega) \cdot \mathbf{n} < 0} \frac{K(\Lambda)}{\Lambda^2} \mathbf{s}(\Omega) \cdot \mathbf{n} d\Omega d\Lambda}, \quad (2)$$

where  $\mathbf{n}$  is the normal to the pore surface and  $\mathbf{J}(\mathbf{r}, \Lambda, \Omega) = \frac{K(\Lambda)}{\Lambda} T(\mathbf{r}, \Lambda, \Omega) \mathbf{s}(\Omega)$  is the thermal flux. The presence

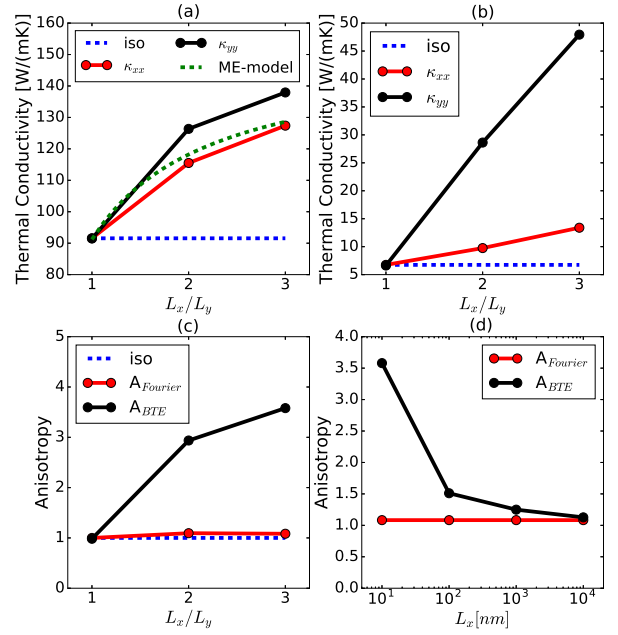


FIG. 2. a) Thermal conductivity tensor for different shape ratio  $r$  and fixed pore-size, computed by the diffusive heat conduction equation. The green-dotted line refers to the analytical case computed according to Maxwell-Garnett theory. b) Thermal conductivity tensor for different  $r$  computed by the BTE. The strong anisotropy is due to the directionality of the characteristic length. c) The anisotropy of thermal conductivity tensor for the cases when phonon size effects are switched on ( $A_{BTE}$ ) and off ( $A_{Fourier}$ ). d) Anisotropy of thermal conductivity tensor for different pore size  $L_x$  and fixed shape ratio  $r = 2$ .

of phonon-boundary scattering results in a strong reduction in thermal transport. For example, for  $r = 1$ ,  $\kappa_{xx} = \kappa_{yy} = 6 \text{ Wm}^{-1}\text{K}^{-1}$ , almost two orders of magnitudes smaller than that in the bulk counterpart [24].

As shown in Fig. 2(c), for larger  $r$  we observe an increasing anisotropy, which amounts to 3.5 for  $r = 3$ . This finding can be explained if we note that for anisotropic pore lattices, the characteristic length  $L_c$  depends on the direction of the applied temperature. For  $r > 1$ , phonons travelling along  $\hat{y}$  experience a larger  $L_c$  than that related to phonons traveling along  $\hat{x}$ . When heat transport is dominated by boundaries, the thermal conductivity goes with  $L_c$  [4], i.e.  $\kappa_{xx}(r) \approx L_c f(\phi(r)) \kappa_{sg}$ , where  $\kappa_{sg}$  is the small grain thermal conductivity [25], hence, directionality in  $L_c$  translates into anisotropic thermal transport. For very large  $r$ , heat transport along  $x$  remains ballistic, as  $L_c$  is fixed, while phonons travelling along  $\hat{y}$  are mainly in the diffusive regime, with the thermal conductivity being  $\kappa_{yy} \approx f(\phi(r)) \kappa_{bulk}$ . Consequently, when  $L_x \gg L_y$ , the anisotropy approaches a plateau, as shown in Fig. 2(c). Fig. 1-(b) shows the magnitude of thermal flux when a temperature gradient is applied along  $\hat{x}$ . As expected, high-flux regions are located in the spaces between the pores along  $\hat{x}$ , i.e. the phonon bottleneck discussed above. As shown by the flux streamlines, phonons tend to travel more uniformly within the inter-pore spaces along  $\hat{y}$ , revealing that, for large  $r$ , pores belonging to different columns do not interact with each other and any further reduction in heat transport is solely due to the decrease in porosity. We note that the pore-pore distance along  $\hat{y}$  can be arbitrarily decreased by choosing  $r < 1$ , potentially achieving higher directionality. The case with ultrasmall phonon necks will be discussed in next section, where we consider configurations with fixed porosity, that is a scenario appealing to thermoelectrics [26]. In fact, if we assume that electrons travel mainly diffusively due to their small MFPs [27], the electrical conductivity is largely influenced by the amount of material removal rather than the actual pores arrangement. Consequently, we may potentially achieve simultaneously low thermal conductivities and good electrical properties, an essential requirement for high-efficiency thermal energy conversion [1]. We consider the fixed porosity  $\phi = 0.25$ , which is ensured by changing the pore size accordingly. When  $r$  increases, the phonon neck along  $x$  shrinks thus the thermal conductivity decreases. The relative suppression of heat transport with respect to the isotropic case is magnified when phonon size effects are included in the calculations, as shown in Fig. 3(a)-(b). On the other side,  $\kappa_{yy}$  increases with  $r$  as the pore-pore distance increases, similarly to the case with fixed pore size. Remarkably, as shown in Fig. 3(c), the anisotropy achieved when size effects are included is about 23, more than an order of magnitude higher than that calculated by the diffusive theory. Furthermore, from Fig. 1(c) we note that phonons contributing to  $\kappa_{xx}$  travel mainly through direct paths, as a consequence of the small bottleneck. This “phonon focusing” effect can be suitable for coupling a heat source with a nanowire, as proposed in a recent study [28]. We

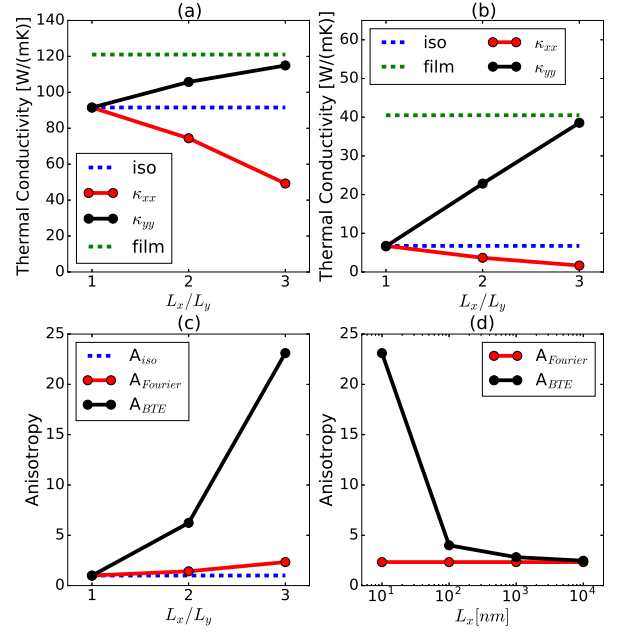


FIG. 3. Thermal conductivity tensor for different shape ratio  $r$  and fixed porosity  $\phi = 0.25$ , computed by the diffusive heat conduction equation. The green-dotted line refers to the thin-film limit. The blue-dotted line represents the analytical case computed by means of the Maxwell-Garnett theory. The thermal conductivity tensors are computed by means of a) diffusive heat conduction and b) BTE. c) The anisotropy of thermal conductivity tensor for the cases when size effects are switched on ( $A_{BTE}$ ) and off ( $A_{Fourier}$ ).

also analyze the “thin film” limit, in which the pores collapse into infinitely extended columns that prevent heat from flowing along  $\hat{x}$ . In this regime, only  $\kappa_{yy}$  survives; this is equivalent to the in-plane thermal conductivity of a thin film with its boundaries scattering phonons diffusively. This regime, which occurs for the shape ratio  $r = 1/\phi = 4$ , provides an upper limit  $\kappa_{yy}$  as also shown in Fig. 3(b). The thermal flux, shown in Fig. 1(d), is higher in the middle of the sample as a result of the scattering between phonons and the boundary of the thin film.

In summary, we have computed the thermal conductivity tensor of porous Si with anisotropic pore lattices, demonstrating that phonon size effects can induce significant anisotropy. The calculations were based on a recently developed method, which computes phonon-size effects with no input parameters rather than the material’s geometry and crystal structure. As these results apply when the constituting material is either isotropic or anisotropic, our findings suggest a practical route to artificially induce or suppress thermal transport directionality, an appealing capability for modern applications such as thermoelectrics and heat management in electronic devices.

## ACKNOWLEDGMENTS

The authors thank Dr. Alexei Maznev for helpful discussions. Research supported as part of the Solid-State Solar-Thermal Energy Conversion Center (S3TEC), an Energy Frontier Research Center funded by the U.S. Department of Energy (DOE), Office of Science, Basic Energy Sciences (BES), under Award DESC0001.

---

\* [romanog@mit.edu](mailto:romanog@mit.edu)

- [1] D. M. Rowe, ed., *CRC Handbook of Thermoelectrics* (CRC Press, Boca Raton, FL, 1995).
- [2] E. Pop, *Nano Research* **3**, 147 (2010).
- [3] W. Kim, R. Wang, and A. Majumdar, *Nano Today* **2**, 40 (2007).
- [4] G. Chen, *Nanoscale energy transport and conversion: a parallel treatment of electrons, molecules, phonons, and photons* (Oxford University Press, USA, 2005).
- [5] R. Venkatasubramanian, E. Siivola, T. Colpitts, and B. O'Quinn, *Nature* **413**, 597 (2001).
- [6] A. I. Boukai, Y. Bunimovich, J. Tahir-Kheli, J.-K. Yu, W. A. Goddard III, and J. R. Heath, *Nature* **451**, 168 (2008).
- [7] A. I. Hochbaum, R. Chen, R. D. Delgado, W. Liang, E. C. Garnett, M. Najarian, A. Majumdar, and P. Yang, *Nature* **451**, 163 (2008).
- [8] D. Song and G. Chen, *Appl. Phys. Lett.* **84**, 687 (2004).
- [9] J. Lee, J. Lim, and P. Yang, *Nano Lett.* (2015).
- [10] J. Tang, H.-T. Wang, D. H. Lee, M. Fardy, Z. Huo, T. P. Russell, and P. Yang, *Nano Lett.* **10**, 4279 (2010).
- [11] P. E. Hopkins, C. M. Reinke, M. F. Su, R. H. Olsson, E. A. Shaner, Z. C. Leseman, J. R. Serrano, L. M. Phinney, and I. El-Kady, *Nano Lett.* **11**, 107 (2011).
- [12] G. Romano and J. C. Grossman, *Appl. Phys. Lett.* **105**, 033116 (2014).
- [13] H. Goldsmid, *Journal of electronic materials* **40**, 1254 (2011).
- [14] M. Zeraati, S. M. V. Allaei, I. A. Sarsari, M. Pourfath, and D. Donadio, *Physical Review B* **93**, 085424 (2016).
- [15] R. Fei, A. Faghaninia, R. Soklaski, J.-A. Yan, C. Lo, and L. Yang, *Nano letters* **14**, 6393 (2014).
- [16] G. Romano and J. C. Grossman, *J. Heat Transf.* **137**, 071302 (2015).
- [17] F. Yang and C. Dames, *Phys. Rev. B* **87** (2013).
- [18] G. Romano, A. Di Carlo, and J. C. Grossman, *J. Comput. Electron.* **11**, 8 (2012).
- [19] C.-W. Nan, R. Birringer, D. R. Clarke, and H. Gleiter, *J. Appl. Phys.* **81**, 6692 (1997).
- [20] D. Broido, M. Malorny, G. Birner, N. Mingo, and D. Stewart, *Appl. Phys. Lett.* **91**, 231922 (2007).
- [21] K. Esfarjani, G. Chen, and H. T. Stokes, *Phys. Rev. B* **84**, 085204 (2011).
- [22] G. Romano and A. Di Carlo, *IEEE Transactions on Nanotechnology* **10**, 1285 (2011).
- [23] T. Abe, *Journal of Computational Physics* **131**, 241 (1997).
- [24] G. Romano, K. Esfarjani, D. A. Strubbe, D. Broido, and A. M. Kolpak, *Physical Review B* **93**, 035408 (2016).
- [25] W. Li, J. Carrete, N. A. Katcho, and N. Mingo, *Computer Physics Communications* **185**, 1747 (2014).
- [26] C. Vineis, A. Shakouri, A. Majumdar, and M. Kanatzidis, *Adv. Mater.* **22**, 3970 (2010).
- [27] B. Liao, B. Qiu, J. Zhou, S. Huberman, K. Esfarjani, and G. Chen, *Phys. Rev. Lett.* **114**, 115901 (2015).
- [28] R. Anufriev, A. Ramiere, J. Maire, and M. Nomura, *arXiv preprint arXiv:1609.08003* (2016).